

Mie Scattering From Micron-Scale Particles

Gerardo F. Salazar

PHY353L Laboratory, Department of Physics, The University of Texas at Austin

Abstract

We constructed an optical apparatus to focus incoming light from a Helium-Neon laser and scatter it off of one-micron diameter latex spheres suspended in water. By adjusting the angular direction of the light via a half-wave plate while holding polarization fixed we were able to isolate both in-plane and out-of-plane scattering intensities. We were able to verify the qualitative predictions of the theory, the phase-shifts, but not the intensity ratios.

1 Introduction

1.1 Background

Mie scattering refers to the scattering of light (in the form of electromagnetic plane waves) from spherical surfaces in the regime where the wavelength of the incident light is much smaller than the diameter of the scattering surface. The original formulation of the theory is due to Gustav Mie (1868-1957) and its modern form is a general theory for predicting scattering properties from spherical targets.

Mie scattering and related theories are responsible for some of nature's most interesting visuals. The color-gradient of the sky at sunset and the dark gray color of clouds on a rainy day are both consequences of this kind of light scattering phenomenon. Our experiment aims to verify the predictions of light-scattering theory detailed below for one set of fixed parameters in two orthogonal directions.

1.2 Theory

The full scattering theory of electromagnetic waves is beyond the scope of this paper. For a detailed presentation of the full theory see [1]. In its place, we will present the key results of the theory in the case of the scatterer having spherical symmetry and its implications to our measurements.

For incident electromagnetic plane waves on a spherical surface the scattered electric field is given by

$$E_{sc} = \frac{i}{K_0 r} e^{iK_0 r} E_0 \left[S_2(\beta, \theta) \cos \phi(\hat{\theta}) + S_1(\beta, \theta) \sin \phi(-\hat{\phi}) \right] \quad (1)$$

Where $K_0 = 2\pi n_m / \lambda$, n_m is the refractive index of the sphere, $\beta = K_0 a$, and a is the sphere diameter. Here S_1 and S_2 are the scattering amplitudes corresponding to the $\hat{\theta}$ and $\hat{\phi}$ directions respectively (out of plane and in plane). They are given by

$$S_1(\beta, \theta) \equiv \sum_{l=1}^{\infty} \frac{2l+1}{l(l+1)} [a_l(\beta) \pi_l(\cos \theta) + b_l(\beta) \tau_l(\cos \theta)] \quad (2)$$

$$S_2(\beta, \theta) \equiv \sum_{l=1}^{\infty} \frac{2l+1}{l(l+1)} [b_l(\beta) \pi_l(\cos \theta) + a_l(\beta) \tau_l(\cos \theta)] \quad (3)$$

Where $a_l(\beta)$ and $b_l(\beta)$ measure the strength of the electric and magnetic multipole radiation respectively and are determined by boundary conditions. Additionally $\pi_l(\cos \theta)$ and $\tau_l(\cos \theta)$ are angular functions defined for convenience as

$$\pi_l(\cos \theta) \equiv \frac{P_l^1(\cos \theta)}{\sin \theta} \quad (4)$$

$$\tau_l(\cos \theta) \equiv \frac{dP_l^1(\cos \theta)}{d\theta} \quad (5)$$

Where P_l^m are associated Legendre polynomials of type (l, m) . The scattering intensities, which is what we plan to measure, are given by $|S_1(\beta, \theta)|^2$ and $|S_2(\beta, \theta)|^2$ and can be calculated using [2]. The exact values of the intensities are sensitive to many experimental parameters but the ratio of the scattering amplitudes is a firm prediction we can verify. Additionally, the $\hat{\theta}$ and $\hat{\phi}$ terms are modulated by $\cos \phi$ and $\sin \phi$ respectively which predicts that the maxima of the scattering intensities should be $\pi/2$ radians out of phase.

2 Experimental Setup

2.1 Apparatus

Broadly, the apparatus consists of a light source, scattering surface, detector, and interface. The light source is a Helium-Neon laser (632.8 nm) behind a modulator connected to the interface for noise reduction. The light of the laser impacts a mirror positioned at 45° so as to reflect the light directly downward into the vessel holding the scattering surface. The scattering surface consists of latex spheres $1.00\mu\text{m} \pm .05\mu\text{m}$ in diameter suspended in water. The water sits under a layer of oil to prevent evaporation. The detector is a photodiode connected to the input of the interface. The photodiode aperture is covered by a polarizer. The function of each of the key components is discussed in more detail below.

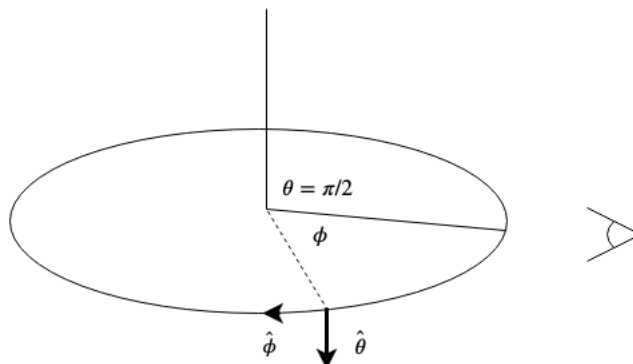


Figure 1: Geometry Near Detector. See Eq.1

2.1.1 Modulator and Interface

The modulator device serves to provide data to the interface so that it may (very successfully) mitigate noise from the input signal. The modulator consists of a spinning wheel with wide slits attached to a motor. The laser sits behind the spinning wheel. As the motor rotates the laser is blocked and unblocked as the slits in the spinning wheel rotate across the plane perpendicular to the laser's propagation. The motor/spinning wheel device has an internal sensor tracking and reporting rotation frequency (ω') to the interface. This allows the interface to perform a transformation of the time series intensity data of the form [3]

$$\int_T \sin(\omega t) \sin(\omega' t) dt \quad (6)$$

Where T is a user selected data acquisition time-window. The transformation allows the interface to effectively pick out the frequency in the input data corresponding to the signal of the laser and output its amplitude. This device is commonly known as a “lock-in amplifier” as the transformation operation allows it to “lock-in” to the laser signal in noisy data.

2.1.2 Half-Wave Plate

The function of the half-wave plate is to change the orientation of an incoming wave. It does so by passing the light through a material with different indices of refraction along perpendicular axes. The result is that one of the orthogonal components of the incident wave is retarded by half of a wavelength, hence the name “half-wave” plate. This results in an effective rotation of the incoming wave by 2θ where θ is the angle of rotation of the half-wave plate. Rotating the half-wave plate allows us to probe the full angular extent of an incident wave.

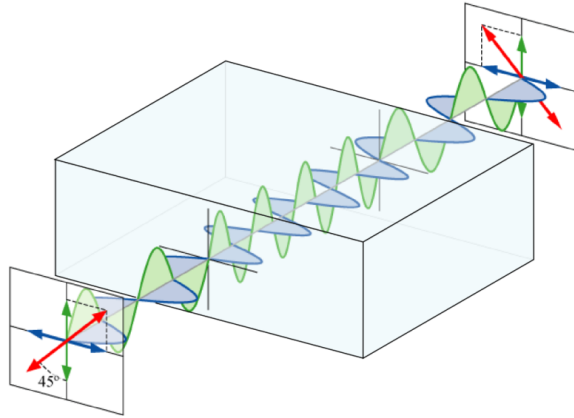


Figure 2: Light Passing Through A Half-Wave Plate [5]

2.1.3 Polarizer

Polarizers serve to strip incoming light waves down to a single direction. Grid polarizers like the one below consist of a large number of very small slits. Incoming light, in the direction of the slits, is absorbed and reflected by the material. Incoming light, in the direction perpendicular to the slits, is transmitted through the slits. The polarizer in front of the photodiode detector allows us to pick which direction of light we are measuring, in plane or out of plane ($\hat{\phi}$ or $\hat{\theta}$).

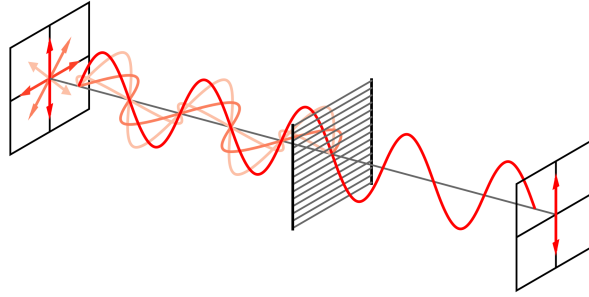


Figure 3: Light Passing Through A Horizontal Polarizer [6]

2.1.4 Photodiode

Laser light on its own does not a physical measurement make. Fortunately, the photodiode detector converts incoming light into an electrical current we can measure. It does so through the so-called “interior” photoelectric effect. The incident photons strike the diode which then, through photoelectric processes, ejects an electron and creates an electron hole. The resulting potential difference creates a current. This current is fed to the interface which uses it to calculate and output a signal amplitude. To good approximation, the resulting current is proportional to the incident light intensity [4]. The exact dependence varies with the properties of the diode.

2.2 Data Collection

The data was collected by fixing the orientation of the polarizer covering the photodiode to isolate either the $\hat{\theta}$ or $\hat{\phi}$ directions of the incident light. In our case, this corresponds to the polarizer being set to 20° and 110° respectively. We then varied the orientation of the half-wave plate through a range $\phi \in [0, 360]$. The intensity was configured to output at a rate of once per second. The interface time-averaged the relevant signal for us and output the result, which we recorded.

3 Analysis and Results

Recall that the predictions of Mie theory that we are testing are the sinusoidal characteristic of the intensity pattern, the $\pi/2$ phase shift between in-plane and out-of-plane direction waveforms, and the in-plane to out-of-plane intensity ratio as given by [2]. We are effectively testing Mie theory at a particular point specified by the polar angle ($\theta = \pi/2$), size parameter ($a = 1\mu\text{m}$), and wavelength ($\lambda = 632.8\text{nm}$). Below is the raw data collected from the interface.

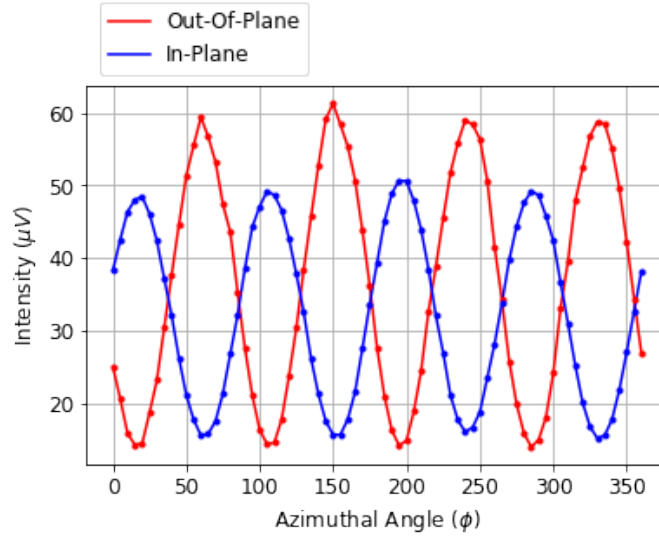


Figure 4: Measured Intensities Of Scattered Light As A Function Of Azimuthal Angle ϕ

Qualitatively, the result matches theory well. Both directions are sinusoidal and look to be a half-period out of phase. Theory predicts that the minima of the waveforms should sit at 0. This can likely be attributed to the spatial extent of the photodiode detector surface absorbing light from more than just one plane. Both waveforms were fit to the following expression

$$I = a \cos^2(\phi + \phi') + b \quad (7)$$

Theory predicts a 90° phase shift, because the cosine fits have opposite amplitude parity this corresponds to identical phase shift terms ϕ' . The difference is given by

$$\phi_O - \phi_I = (90.4 \pm .2) - (89.5 \pm .1) = .9 \pm .2$$

This reflects theory within 1%, which is within the error of the measurements provided by the photodiode (during calibration we noted that ambient light contributed more than 1% to the total measurement).

The amplitude ratio at min-max pairs of the waveforms is predicted to be (for sphere index of refraction $n_S = 1.52$ and medium index of refraction $n_M = 1.33$) is 2.66. The value given by the waveforms is 3.9. Clearly, this is far from agreement. This value, however,

depends on many of the physical parameters we were unable to feasibly measure (E_0 , m_S , distance to detectors, etc.).

4 Conclusion

By constructing an optical device to isolate in-plane and out-of-plane directions of light scattered by large (in comparison to the wavelength of light) spheres we were able to verify predictions of Mie theory at a fixed polar angle, size parameter, and wavelength. The predictions verified were the sinusoidal relationship of the intensity amplitudes and the 90° phase-shift difference between in-plane and out-of-plane waveforms.

Additional testing could be done by varying the three aforementioned parameters. Increased accuracy could be gained from a laboratory free of light pollution as well as limiting the spatial extent of the detector surface.

References

- [1] Grandy, Walter. *Scattering of Waves from Large Spheres*. Ch. 3. Cambridge University Press, 2000.
- [2] Reilly, Christopher. Mie Scattering Calculator.
<http://chris.reillybrothers.net/mie.html>
- [3] Stanford Research Systems. *Model SR380 DSP Lock-In Amplifier Manual*.
<https://www.thinksrs.com/mult/sr810830m.html>. (Retrieved 7/10/2019)
- [4] Haberlin, Heinrich. *Photovoltaics: System Design and Practice*. John Wiley & Sons, 2012.
- [5] CC BY-SA 3.0,
<https://commons.wikimedia.org/w/index.php?curid=12105328>
- [6] CC BY-SA 3.0,
<https://commons.wikimedia.org/w/index.php?curid=724493>